Article

On the Mechanism of THF Catalyzed Vinylic Lithiation of Allylamine Derivatives: Structural Studies Using 2-D and Diffusion-Ordered NMR Spectroscopy

Madeleine A. Jacobson, Ivan Keresztes, and Paul G. Williard

J. Am. Chem. Soc., **2005**, 127 (13), 4965-4975• DOI: 10.1021/ja0479540 • Publication Date (Web): 11 March 2005

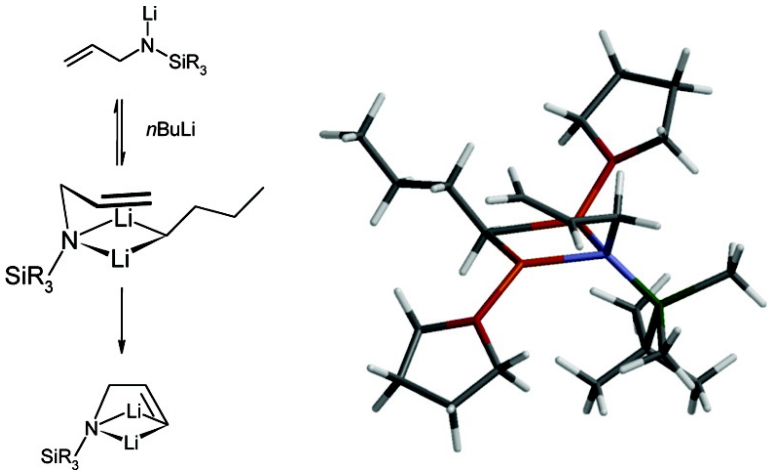

More About This Article

Additional resources and features associated with this article are available within the HTML version:

- Supporting Information
- Links to the 10 articles that cite this article, as of the time of this article download
- Access to high resolution figures
- Links to articles and content related to this article
- Copyright permission to reproduce figures and/or text from this article

View the Full Text HTML

J|A|C|S
ARTICLES
Published on Web 03/11/2005

On the Mechanism of THF Catalyzed Vinylic Lithiation of Allylamine Derivatives: Structural Studies Using 2-D and Diffusion-Ordered NMR Spectroscopy

Madeleine A. Jacobson, Ivan Keresztes, and Paul G. Williard*

Contribution from the Department of Chemistry, Brown University, Providence, Rhode Island 02912

Received April 8, 2004; E-mail: Paul_Williard@brown.edu

Abstract: *N*-Lithio-*N*-(trialkylsilyl)allylamines can be deprotonated in the presence of ethereal solvents exclusively at the *cis*-vinylic position to yield 3,*N*-dilithio-*N*-(trialkylsilyl)allylamines under mild conditions. Low temperature ^{1}H and ^{7}Li NMR (^{1}H NOESY, TOCSY, ^{1}H/^{7}Li HSQC, and DO-NMR) studies on the solution structure of 3,*N*-dilithio-*N*-(*tert*-butyldimethylsilyl)allylamine identified three major aggregates in THF (monomer, dimer and tetramer), but the aggregate structures failed to explain the solvent dependence and regiochemical outcome of the reaction. Low temperature ^{1}H NMR (NOESY, TOCSY, DO-NMR) studies on the solution structure of *N*-lithio-*N*-(*tert*-butyldimethylsilyl)allylamine in the presence of *n*BuLi identified amide/*n*BuLi mixed aggregates in both the ethereal solvent THF (1:1 dimer) and the hydrocarbon solvent toluene (1:3 tetramer). Addition of 2 equiv of THF to toluene solutions induces the formation of the same THF solvated 1:1 dimer as observed in neat THF. NMR evidence suggests that in THF the mixed aggregate has close contact between the olefin and the β-CH_2 of *n*BuLi, while in the absence of THF, the allyl chain appears to be pointed away from the nearest *n*BuLi residues.

Introduction

It has been known for some time that many organolithium compounds form mixed aggregates, both with other organolithiums and with inorganic lithium salts. However, it is only in the past decade that the importance and utility of mixed aggregates in organic chemistry have been recognized.[1] The primary way to study these mixed aggregates, and investigate structure−reactivity relationships, is by NMR. Some questions of particular interest are how addition of coordinating solvents, as well as the choice of primary solvent—ethereal or hydrocarbon—affects the aggregation state and the composition of the aggregates in solution. The effect of lithium salts on aggregate structures has also been studied.[2] The groups of Collum,[3] Hilmersson,[4] Thomas,[5] van Koten,[6] Klumpp,[7] Chabanel,[8] and Duhamel[9] have all independently carried out extensive studies on the solution structure and stereochemistry of mixed aggregates. It is well-established that mixed aggregates containing organolithium starting materials and lithium-containing products can cause marked dependencies of reactivities and selectivities on the organolithium/substrate ratios.[1c,10] The X-ray structure[11]

(1) For discussion of, and leading references to, mixed aggregates, see (a) Kremer, T.; Harder, S.; Junge, M.; Schleyer, P. von R. *Organometallics* **1996**, *15*, 585−595. (b) Jackman, L. M.; Rakiewicz, E. F. *J. Am. Chem. Soc.* **1991**, *113*, 1202−1210. (c) Seebach, D. *Angew. Chem., Int. Ed. Engl.* **1988**, *27*, 1624−1654. For investigations of RLi/OLi mixed aggregation, see (d) Saá, J. M.; Martorelli, G.; Frontera, A. *J. Org. Chem.* **1996**, *61*, 5194−5195. (e) Balamraju, Y.; Sharp, C. D.; Gammil, W.; Manuel, N.; Pratt, L. M. *Tetrahedron* **1998**, *54*, 7357−7366. (f) Marsch, M.; Harms, K.; Lochmann, L.; Boche, G. *Angew. Chem., Int. Ed. Engl.* **1990**, *29*, 308−309. (g) McGarrity, J. F.; Ogle, C. A. *J. Am. Chem. Soc.* **1985**, *107*, 1805−1810. (h) McGarrity, J. F.; Ogle, C. A. *J. Am. Chem. Soc.* **1985**, *107*, 1810−1815. (i) Darensbourg, M. Y.; Kimura, B. Y.; Hartwell, G. E.; Brown, T. L. *J. Am. Chem. Soc.* **1970**, *92*, 1236−1242. (j) Setiz, L. M.; Brown, T. L. *J. Am. Chem. Soc.* **1966**, *88*, 2174−2178. (k) Lochmann, L.; Pospisil, J.; Vodnansky, J.; Trekoval, J.; Lim, D. *Collect. Czech. Chem. Commun.* **1965**, *30*, 2187−2195. For theoretical investigations of RLi/Oli mixed aggregates, see (l) Sorger, K.; Schleyer, P. von R.; Stalke, D. *J. Am. Chem. Soc.* **1996**, *118*, 6924−6933. (m) Morey, J.; Costa, A.; Deyá, P. M.; Suner, G.; Saá, J. M. *J. Org. Chem.* **1990**, *55*, 3902−3909.

(2) For an example of a LiBr/chelating alkoxide mixed aggregate, see (a) van der Schaaf, P. A.; Hogerheide, M. P.; Grove, D. M.; Spek, A. L.; van Koten, G. *J. Chem. Soc., Chem. Commun.* **1992**, 1703−1705. For examples of an acetylide/LiBr mixed aggregate, see (b) Reich, H. J.; Eisenhart, E. K.; Olson, R. E.; Kelly, M. J. *J. Am. Chem. Soc.* **1986**, *108*, 7791−7800.

(3) For some recent examples, see: (a) Zhao, P.; Collum, D. B. *J. Am. Chem. Soc.* **2003**, *125*, 4008−4009. (b) Parsons, R. L., Jr.; Fortunak, J. M.; Dorow, R. L.; Harris, G. D.; Kauffman, G. S.; Nugent, W. A.; Winemiller, M. D.; Briggs, T. F.; Xiang, B.; Collum, D. B. *J. Am. Chem. Soc.* **2001**, *123*, 9135−9143. (c) Sun, X.; Winemiller, M. D.; Xiang, B.; Collum, D. B. *J. Am. Chem. Soc.* **2001**, *123*, 8039−8046. (d) Briggs, T. F.; Winemiller, M. D.; Xiang, B.; Collum, D. B. *J. Org. Chem.* **2001**, *66*, 6291−6298. (e) Xu, F.; Reamer, R. A.; Tillyer, R.; Cummins, J. M.; Grabowski, E. J. J.; Reider, P. J.; Collum, D. B.; Huffman, J. C. *J. Am. Chem. Soc.* **2000**, *122*, 11212−11218. (f) Chadwick, S. T.; Rennels, R. A.; Rutherford, J. L.; Collum, D. B. *J. Am. Chem. Soc.* **2000**, *122*, 8640−8647. (g) Sun, X.; Collum, D. B. *J. Am. Chem. Soc.* **2001**, *122*, 2459−2463. (h) Thompson, A.; Corley, E. G.; Huntington, M. F.; Grabowski, E. J. J.; Remenar, J. F.; Collum, D. B. *J. Am. Chem. Soc.* **1998**, *120*, 2028−2038.

(4) (a) Hilmersson, G.; Malmros, B. *Chem.—Eur. J.* **2001**, *7*, 337−341. (b) Arvidsson, P. I.; Hilmersson, G.; Davidsson, Ö. *Chem.—Eur. J.* **1999**, *5*, 2348−2355. (c) Arvidsson, P. I.; Ahlberg, P.; Hilmersson, G. *Chem.—Eur. J.* **1999**, *5*, 1348−1354. (d) Hilmersson, G.; Ahlberg, P.; Davidsson, Ö. *J. Am. Chem. Soc.* **1996**, *118*, 3539−3540.

(5) (a) DeLong, G. T.; Pannell, D. K.; Clarke, M. T.; Thomas, R. D. *J. Am. Chem. Soc.* **1993**, *115*, 7013−7014. (b) Bates, T. F.; Clarke, M. T.; Thomas, R. D. *J. Am. Chem. Soc.* **1988**, *110*, 5109−5112. (c) Thomas, R. D.; Clarke, M. T.; Jensen, R. M.; Young, T. C. *Organometallics* **1986**, *5*, 1851−1857.

(6) Wijkens, P.; van Koten, E. M.; Janssen, M. D.; Jastrzebski, T. B. H.; Spek, A. L.; van Koten, G. *Angew. Chem., Int. Ed. Engl.* **1995**, *34*, 219−222.

(7) Schmitz, R. F.; Dekanter, F. J. J.; Schakel, M.; Klumpp, G. W. *Tetrahedron* **1994**, *50*, 5933−5944.

(8) Goralski, P.; Legoff, D.; Chabanel, M. *J. Organomet. Chem.* **1993**, *456*, 1−5.

(9) Corruble, A.; Valnot, J.-Y.; Maddaluno, J.; Prigent, Y.; Davoust, D.; Duhamel, D. *J. Am. Chem. Soc.* **1997**, *119*, 10042−10048.

(10) (a) Juaristi, E.; Beck, A. K.; Hansen, J.; Matt, T.; Mukhopadhyay, M.; Simson, M.; Seebach, D. *Synthesis* **1993**, 1271−1290. (b) Hall, P.; Gilchrist, J. H.; Collum, D. B. *J. Am. Chem. Soc.* **1991**, *113*, 9571−9574.

and reactivity[12] of a mixed aggregate containing commercially available alkyllithiums and a chiral lithium amide derived from *N*-isopropyl-*O*-methyl valinol, as well as the solution structure of the lithium enolate of 3-pentanone and the same chiral lithium amide, were also investigated.[13] In addition, we have shown that diffusion-ordered NMR (DOSY) can be used to distinguish between different organolithium aggregates in solution.[14] Next, we wish to report our most recent findings concerning the pathway by which we believe a dimeric, mixed aggregate formed in solutions containing ethereal solvents, such as THF, leads to exclusive formation of a vinyllithium anion and not to the alternative allyl anion.

Experimental Procedures

General Methods. *n*-Butyllithium (*n*BuLi) was obtained from Aldrich Chemical Co. (2.5 M in hexanes), and the exact concentration of the solution was determined by direct titration with 2,5-dimethoxybenzyl alcohol in THF. Deuterated NMR solvents were dried over 3 Å Linde sieves prior to use. All reactions and NMR studies were carried out under argon atmosphere, using flame-dried glassware. NMR spectra were collected on Bruker DRX400 or DPX300 spectrometers operating at 400 and 300 MHz for ^{1}H and 100 and 75 MHz for ^{13}C observation. The chemical shifts were referenced to THF-d_8 (^{1}H 1.73 ppm) and toulene-d_8 (^{1}H 2.09 ppm) as internal standards. ^{7}Li chemical shifts were referenced to 0.3 M LiBr in D_2O at 25 °C as an external standard. Sample temperature was calibrated with a standard methanol sample.

Diffusion-Ordered Experiments. Diffusion-ordered experiments were performed on Bruker DRX400 spectrometer equipped with an Accustar *z*-axis gradient amplifier and a QNP probe with a *z*-axis gradient coil. Maximum gradient strength was 0.327 T/m. Bipolar rectangular gradients were used with total durations of 2−5 ms. Gradient recovery delays were 0.5−1 ms. Diffusion times were between 300 and 1000 ms. In LED experiments, the eddy current delays were 3−10 ms. Data processing was accomplished with XWINNMR 2.6, Bruker Inc. Individual rows of the quasi-2-D diffusion datasets were individually phase and baseline corrected. Resonances of interest were integrated, and the integral values were exported into and analyzed in a spreadsheet application.[28]

General Procedure for Preparation of NMR Samples of 4 and 10. A total of 1 equiv of *n*BuLi in hexanes was placed in a flame-dried NMR tube under argon atmosphere. The hexanes were removed in vacuo, and 0.6 mL of THF-d_8 or toulene-d_8 was added. To this clear and colorless solution 1 equiv of **4** was added. Samples of **10** were prepared by adding 0.5 equiv of **4** and allowing the sample to stand at −40 °C for 1 week, at which time dianion formation was complete.

Results

Treatment of allyl alcohol and allylamine derivatives with strong base effects reactions in which synthetically useful allylanions are formed.[15] An alternative to allylic deprotonation is observed with secondary allylamines. These compounds can undergo vinylic deprotonation at the 3-position. This reaction is observed exclusively upon reaction of *N*-monoalkyl and *N*-silyl allylamine with alkyllithium reagents. Several variations of this vinylic anion forming reaction are documented.[16] The vinyllithium reagents generated in this reaction are necessarily formed as dianions with *Z* stereochemistry, exclusively. These *Z*-vinyllithium reagents react with various electrophiles to produce a wide variety of heterocyclic compounds, including borazoles, silylazoles, benzepines, indoles, and pyrroles.[16g,17] Corriu et al.[16g] first noted the relatively mild conditions (2 equiv of *n*BuLi, 0 °C, diethyl ether) required to form the dianion of *N*-(trimethylsilyl)allylamine. We have shown that lithiation does not take place in hydrocarbon solvents even at elevated temperatures, but reactivity is restored upon the addition of catalytic amounts of ethereal solvents.[18] The crystal structures of the 3,*N*-dilithio-*N*-(trimethylsilyl)-, 3,*N*-dilithio-*N*-(triisopropylsilyl)-, and 3,*N*-dilithio-*N*-(*tert*-butyldimethylsilyl)allylamines were reported.[19] In addition, detailed density functional theory studies of the mechanism of regioselective allylic and *cis*-vinylic deprotonation of allyl amides and allyl amines have recently been investigated.[44]

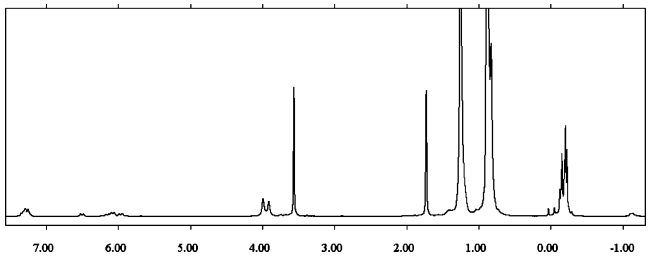

Figure 1. ^{1}H NMR spectrum of 0.1 M solution of **3** containing a small amount of *n*BuLi in THF-d_8 at −80 °C. The truncated peaks arise from hexanes, which were not completely removed during preparation of the sample.

Scheme 1

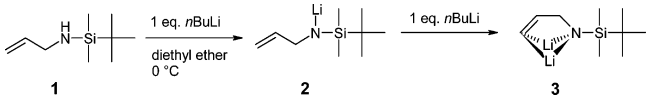

Preliminary NMR work[20] strongly indicated that the dianion derived from **1**, 3,*N*-dilithio-*N*-(*tert*-butyldimethylsilyl)allylamine (**3**), retains the *c*-clamp-like structure observed in the solid state (Scheme 1).[19] Our findings regarding the aggregation behavior of **3** are described next.

Solution State Structure of 3,*N*-Dilithio-*N*-(*tert*-butyldimethylsilyl)allylamine (3). While at room temperature, only a single set of allylic peaks is observed in the ^{1}H NMR spectrum of **3**; at and below −80 °C, the vinylic region of the ^{1}H NMR spectrum displays multiple sets of vinylic resonances (Figure 1). Good peak separation in the region between 5.8 and 6.6 ppm enabled us to identify four major and one minor set of vinylic peaks (Figure 2). In addition, the sample also contained a small amount of *n*BuLi, which showed two partially resolved α-CH_2 signals, and lithium *n*-butoxide (*n*BuOLi), a common impurity in commercial *n*BuLi. One of the *n*BuLi α-CH_2

(11) Williard, P. G.; Sun, C. *J. Am. Chem. Soc.* **1997**, *119*, 11693−11694.
(12) Haeffner, F.; Sun, C.; Williard, P. *J. Am. Chem. Soc.* **2000**, *122*, 12542−12546.
(13) Sun, C.; Williard, P. G. *J. Am. Chem. Soc.* **2000**, *122*, 7829−7830.
(14) Keresztes, I.; Williard, P. G. *J. Am. Chem. Soc.* **2000**, *122*, 10228−10229.
(15) (a) Katritzky, A. R.; Piffl, M.; Lang, H.; Anders, E. *Chem. Rev.* **1999**, *99*, 665−722.
(16) (a) Barluenga, J.; Sanz, R.; Fananás, F. J. *Tetrahedron Lett.* **1997**, *38*, 2763−2766. (b) Yus, M.; Foubelo, F.; Falvello, L. R. *Tetrahedron: Asymmetry* **1995**, *6*, 2081−2092. (c) Barluenga, J. *Pure Appl. Chem.* **1990**, *62*, 595−604. (d) Barluenga, J.; Foubelo, F.; Fananás, F. J.; Yus, M. *J. Chem. Res., Synop.* **1989**, *7*, 200−201. (e) Barluenga, J.; Fananás, F. J.; Foubelo, F.; Yus, M. *J. Chem. Soc., Chem. Commun.* **1988**, *16*, 1135−1136. (f) Burns, S. A.; Corriu, R. J. P.; Huynh, V.; Moreau, J. J. E. *J. Organomet. Chem.* **1987**, *333*, 281−290.
(17) (a) Wrackmeyer, B.; Ordung, I.; Schwarze, B. *Naturforsch. B* **1997**, *52*, 427−430. (b) Corriu, R. J. P.; Geng, B.; Moreau, J. J. E. *J. Org. Chem.* **1993**, *58*, 1443−1448. (c) Smith, A. B., III; Visnick, M. *Tetrahedron Lett.* **1985**, *26*, 3757−3760. (d) Schulze, J.; Boese, R.; Schmid, G. *Chem. Ber.* **1981**, *114*, 1297−1305. (e) Schulze, J.; Schmid, G. *J. Organomet. Chem.* **1980**, *193*, 83−91. (f) Hänssgen, D.; Odenhausen, E. *Chem. Ber.* **1979**, *112*, 2389−2393.
(18) Jacobson, M. A.; Williard, P. G. *J. Org. Chem.* **2002**, *67*, 32−37.
(19) Williard, P. G.; Jacobson, M. A. *Org. Lett.* **2000**, *2*, 2753−2755.
(20) Jacobson, M. A. Ph.D. Thesis, Brown University, 2001.

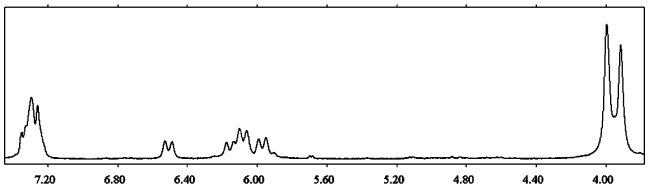

Figure 2. ^{1}H NMR spectrum of 0.1 M solution of **3** containing a small amount of *n*BuLi in THF-d_8 at −80 °C. Downfield expansion plot showing the allylic region of the ^{1}H NMR spectrum.

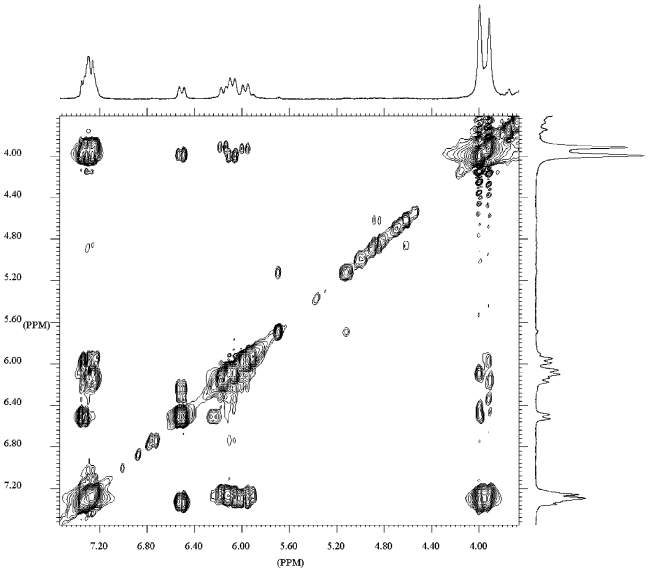

Figure 3. Phase-sensitive 2-D NOESY spectrum of 0.1 M solution of **3** containing a small amount of *n*BuLi in THF-d_8 at −80 °C. Expansion plot of the allylic region showing connectivity within the allylic spin systems.

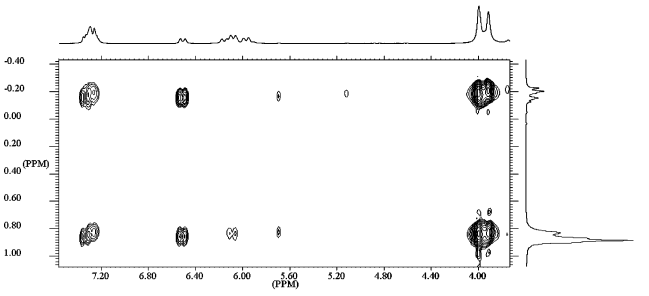

Figure 4. Phase-sensitive 2-D NOESY spectrum of 0.1 M solution of **3** containing a small amount of *n*BuLi in THF-d_8 at −80 °C. Expansion plot showing the connectivity between the allylic and TBDMS resonances.

resonances was assigned to the well-known tetrasolvated dimeric *n*BuLi homoaggregate[21] by chemical shift equivalence to an authentic sample. 2-D COSY and NOESY experiments were used to assign the chemical shifts of all ^{1}H resonances in the corresponding five allylic and two butyl spin systems (Figure 3). To some degree, the assignments could be extended to the TBDMS groups via the nuclear Overhauser effect (Figure 4). Two *n*BuLi residues and the *n*BuOLi showed nOe correlations to TBDMS methyl resonances, indicating that they form parts of mixed aggregates with lithium amide residues. Thus, a total of five aggregates of **3** could be assigned: three homoaggregates (**4**−**6**), an *n*BuLi containing mixed aggregate (**7**), and a mixed aggregate containing one molecule each of **3**, *n*BuLi and *n*BuOLi (**8**) (Scheme 2). Justification for the proposed aggregate structures is presented next, and chemical shifts are summarized in Table 1.

The rigid *c*-clamp conformation imposes a minimum distance of about 5 Å between H-3 and the nearest TBDMS protons within a single molecule of **3**. Because of that distance, nOe correlations cannot arise between the H-3 and TBDMS protons on the same molecule. 2-D NOESY spectra showed no nOe correlations between the H-3 resonances of **4**, **7**, and **8** and the TBDMS region, which, while certainly not unequivocal proof, is consistent with the presence of only a single dianion residue in these aggregates. On the other hand, strong nOe correlations were observed between H-3 and TBDMS resonances of **6** and similar but weaker ones for **5**, indicating that these aggregates contain multiple chemically equivalent dianion residues (Figure 4).

Further information about aggregation numbers was obtained from diffusion-ordered NMR (DO-NMR) experiments.[22] As the name implies, these experiments can be used to measure diffusion coefficients—and thereby physical size—by NMR spectroscopy. The Stokes−Einstein equation relates diffusion coefficients with hydrodynamic radii.[23] Various pulse sequences[24] including hyphenated combination experiments, as well as improved methods of data analysis[25] have been developed. DO-NMR is a rapidly maturing technique, which has been applied to many chemical systems,[26] but only recently penetrated the field of organometallic chemistry.[27] Our group was the first to successfully use DO-NMR to differentiate organolithium aggregates based on their mobility.[14] In these studies, we used the double stimulated echo (DSTE) sequence[24c] with longitudinal eddy current delay[26h] (LED) because of its ability to suppress convection artifacts.

(21) NMR work (a) Bauer, W.; Clark, T.; Schleyer, P. von R. *J. Am. Chem. Soc.* **1987**, *109*, 970−977. (b) Heinzer, J.; Oth, J. F. M.; Seebach, D. *Helv. Chim. Acta* **1985**, *68*, 1848−1862. (c) McGarrity, J. F.; Ogle, C. A. *J. Am. Chem. Soc.* **1985**, *107*, 1805−1810. (d) Seebach, D.; Hässig, R.; Gabriel, J. *Helv. Chim. Acta* **1983**, *66*, 308−337. X-ray work (e) Nichols, M. A.; Williard, P. G. *J. Am. Chem. Soc.* **1993**, *115*, 1568−1572. (f) Barnett, N. D. R.; Mulvey, R. E.; Clegg, W.; O'Neil, P. A. *J. Am. Chem. Soc.* **1993**, *115*, 1573−1574.

(22) (a) Tanner, J. E. *J. Chem. Phys.* **1970**, *52*, 2523−2526. (b) Stejskal, E. O.; Tanner, J. E. *J. Chem. Phys.* **1963**, *42*, 288−292. For recent reviews, see (c) Antalek, B. *Concept Magn. Reson.* **2002**, *14*, 225−258. (d) Johnson, C. S., Jr. *Prog. Nucl. Magn. Reson.* **1999**, *34*, 203−256. (e) Price, W. S. *Concept Magn. Reson.* **1997**, *9*, 299−336.

(23) $D = (k_BT)/(6\pi\eta r)$, where D is the diffusion coefficient, k_B is the Boltzman constant, T is the temperature in Kelvin, η is the viscosity of the solution, and r is the radius of the molecular sphere.

(24) (a) Millet, O.; Pons, M. *J. Magn. Reson.* **1998**, *131*, 166−169. (b) Barjat, H.; Morris, G. A.; Swanson, G. A. *J. Magn. Reson.* **1998**, *131*, 131−138. (c) Jerschow, A.; Müller, N. *J. Magn. Reson.* **1997**, *125*, 372−375. (d) Jerschow, A.; Müller, N. *J. Magn. Reson., Ser. A* **1996**, *123*, 222−225. (e) Chen, A.; Wu, D.; Johnson, C. S., Jr. *J. Am. Chem. Soc.* **1995**, *117*, 7965−7970. (f) Wong, S.; Vasudevan, S.; Vaia, R. A.; Gianellis, E. P.; Zax, D. B. *J. Am. Chem. Soc.* **1995**, *117*, 7568−7569. (g) Altiere, A. S.; Hinton, D. P.; Byrd, R. A. *J. Am. Chem. Soc.* **1995**, *117*, 7566−7567.

(25) For DOSY processing (a) Van Gorkom, L. C. M.; Hancewitcz, T. M. *J. Magn. Reson.* **1998**, *130*, 125−130. (b) Kenkre, V. M.; Fukushima, E.; Sheltraw, D. *J. Magn. Reson.* **1997**, *128*, 62−69. (c) Stilbs, P.; Paulsen, K.; Griffiths, P. C. *J. Phys. Chem.* **1996**, *100*, 8180−8189. (d) Schulze, D.; Stilbs, P. *J. Magn. Reson., Ser. A* **1993**, *105*, 54−58.

(26) For examples of applications, see (a) McCord, D. J.; Small, J. H.; Greaves, J.; Van, Q. N.; Shaka, A. J.; Flesicher, E. B.; Chea, K. J. *J. Am. Chem. Soc.* **1998**, *120*, 9763−9770. (b) Ilyina, E.; Roongta, V.; Pan, H.; Woodward, C.; Mayo, K. H. *Biochemistry* **1997**, *36*, 3383−3388. (c) Potter, K.; Kleinberg, R. L.; Brockman, F. J.; McFarland, E. W. *J. Magn. Reson., Ser. B* **1996**, *113*, 9−15. (d) Lin, M.; Jayawickrama, D. A.; Rose, R. A.; DelViscio, J. A.; Larive, C. K. *Anal. Chim. Acta* **1995**, *307*, 449−457. (e) Young, J. K.; Baker, G. R.; Newkome, G. R.; Morris, K. F.; Johnson, C. S., Jr. *Macromolecules* **1994**, *27*, 3464−3471. (f) Hinton, D. P.; Johnson, C. S., Jr. *Chem. Phys. Lipids* **1994**, *69*, 175−178. (g) Hinton, D. P.; Johnson, C. S., Jr. *J. Phys. Chem.* **1993**, *97*, 9064−9072. (h) Gibbs, S. J.; Johnson, C. S., Jr. *J. Magn. Reson.* **1991**, *93*, 395−402.

(27) (a) Pichota, A.; Pregosin, P. S.; Valentini, M.; Worle, M.; Seebach, D. *Angew. Chem., Int. Ed.* **2000**, *39*, 153−156. (b) Valentini, M.; Pregosin, P. S.; Ruegger, H. *Organometallics* **2000**, *19*, 2551−2555. (c) Beck, S.; Geyer, A.; Brintzinger, H. *J. Chem. Soc., Chem. Commun.* **1999**, 2477−2478.

Scheme 2

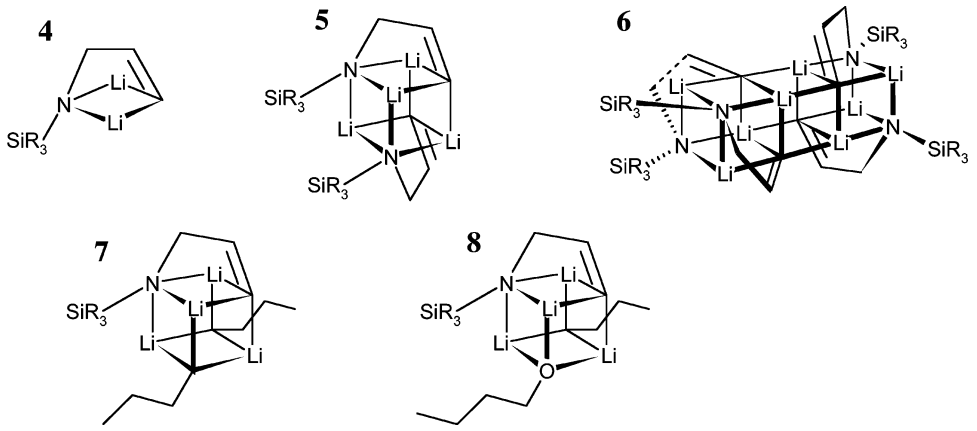

Table 1. ^{1}H Chemical Shifts[a] of Lithium Amide Containing Aggregates in THF-d_8 at −80 °C

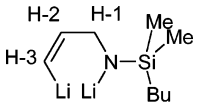

3

	lithium amide					*n*BuLi		
	4	**5**	**6**	**7**	**8**		**7**	**8**
H-1	3.91	4.00	3.99	3.93	3.94	α	−1.14	−1.18
H-2	6.15	6.08	6.51	5.97	5.92	*β*	1.44	1.43
H-3	7.26	7.28	7.34	7.31	7.25	*γ*	1.18	1.18
Bu	N/D	0.83	0.86	0.85	N/D	*δ*	0.82	0.82
Me	N/D	−0.19	−0.15	−0.20	N/D	nOe[b]	−0.20	−0.16

[a] In ppm, derived from 2-D TOCSY and NOESY experiments. [b] nOe correlation from *n*BuLi to lithium amide silyl methyl group.

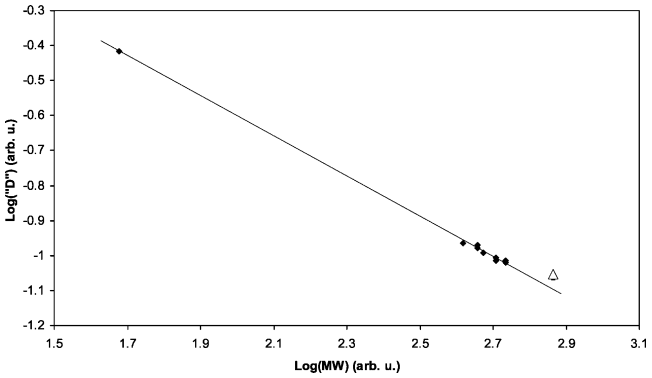

Figure 5. DO-NMR of the major aggregates at −80 °C. The solid line is linear least-squares fit to the data points represented by diamonds. The triangle represents the tetramer **6** and was not included in the fit.

Our current approach[28] for solutions containing mixtures of aggregates is to estimate the molecular weight (MW) of each aggregate by correlating their experimentally determined mobility and expected MW. Success of this method requires additional information regarding the structure of at least some of the aggregates so that educated guesses can be made regarding possible MW values. We use the solvent and aggregates of known composition as internal references, whenever possible. In this case, we used the MW of the *n*BuLi dimer in conjunction with residual THF-d_7 as our starting point for correlating experimental mobilities and MWs. The MWs were then adjusted

(28) Keresztes, I. Ph.D. Thesis, Brown University, 2001.

Table 2. DO-NMR of the Aggregates in THF-d_8 at −80 °C

	4	**5**	**6**	**7**	**8**	(*n*BuLi)$_2$
3	1	2	4	1	1	0
*n*BuLi	0	0	0	2	1	2
*n*BuOLi	0	0	0	0	1	0
THF	5	2	0	2	2	4
MW	543	510	732	455	471	416

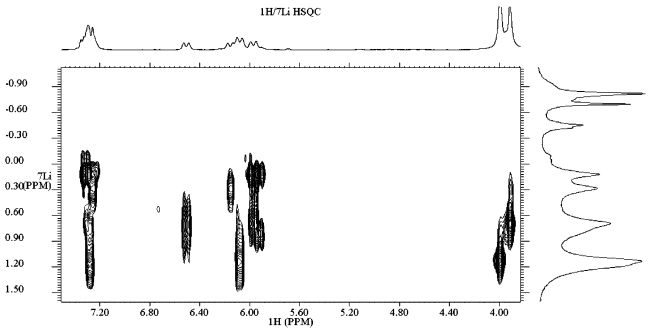

Figure 6. Phase-sensitive ^{1}H/^{7}Li HSQC spectrum of 0.1 M solution of **3** containing a small amount of *n*BuLi in THF-d_8 at −80 °C.

by varying the number of lithium amide residues in the homoaggregates and the composition and number of coordinated THF ligands in all aggregates, until the best possible correlation was obtained (Figure 5 and Table 2). All proposed structures were confirmed to be minima on the potential energy surface by PM3 semiempirical calculations.[29] The best fit for the higher order aggregate **6** actually corresponded to a monosolvated trimer. While such a structure remains a possibility, we propose the unsolvated tetramer because **6** has only a single set of resonances in ^{1}H NMR spectra. We cannot envision a reasonable trimeric structure with three equivalent dianion sites. In addition, X-ray crystallographic evidence shows that the proposed tetrameric structure is available to these dianions.[19] Deviation from the calibration curve is attributed to the cylindrical shape of the tetrameric aggregate. Unambiguous assignment of the aggregation state of the higher order aggregate **6** was deemed beyond the scope of this work.

Additional proof of these structures was obtained from the ^{1}H/^{7}Li HSQC spectrum (Figure 6, Table 3). To the best of our knowledge, this is the first published example where the ^{1}H/^{7}-

(29) PM3: Stewart, J. J. P. *J. Comput. Chem.* **1989**, *10*, 209−220. Li parameters: Anders, E.; Koch, R.; Freunscht, P. *J. Comput. Chem.* **1993**, *14*, 1301−1312. The calulations were performed with PC Spartan Pro, Wave function Inc. 18401 Von Karman Ave., Suite 370, Irvine, CA 92715.

Li pair of nuclei was correlated via scalar coupling. We found that $^1H/^7Li$ chemical shift correlation experiments via two and three bond scalar couplings are generally attainable even in the absence of resolved coupling. Details of this work will be communicated elsewhere.[30] While ^1H/metal chemical shift correlations have been used extensively in the structure determination of organometallic compounds, only a few $^1H/^6Li$ correlation experiments have been previously reported.[12a,31] It should be noted that heteronucleus and inverse detected 2-D experiments based on dipolar coupling (HOESY) have been used with great success for both $^1H/^6Li$ and $^1H/^7Li$ pairs of nuclei.

In agreement with the proposed monomeric structure, the aggregate **4** showed correlations to only a single ^7Li chemical shift from all allylic protons. The dimeric aggregate **5**, which has two different lithium sites, actually showed correlations to three different ^7Li chemical shifts. However, given the large ^7Li line widths, it would be impossible to distinguish between a single correlation to H-2 at 1.82 ppm and two separate correlations at 1.80 and 1.86. We observed only a single, very broad correlation for the tetramer **6**. Attempts to assign further lithiums to this aggregate via intraaggregate lithium exchange (EXSY) failed. The mixed aggregates both showed correlations to the same lithium from H-1 and H-3 as well as H-2 and H-3. In addition, correlations were observed between lithium resonances and the α-CH_2 resonances.

In the course of this work, we uncovered a wide variety of structural variations in the aggregation behavior of **3**. There is, however, a single unifying feature in all structures: individual molecules of **3** adopt the same *c*-clamp shape conformation (Scheme 1) in the solid[19] and solution state, in monomeric, higher order, and mixed aggregates and with or without coordinating solvents.

It would seem convenient to suggest that the stability of the *c*-clamp structure, which is preserved in all aggregates identified both in the solid and in the solution state, accounts for the regiospecificity of these reactions. In other words, the reaction is under thermodynamic control, and the regiochemical outcome is driven by the stability of the resulting dianion.

Computational results suggest that the allylic dianion, which would result from deprotonation at the C-1 position, could adopt a very similar bicyclic *c*-clamp structure with two lithium atoms bridging the terminal carbon and the nitrogen (Scheme 3). This

Scheme 3

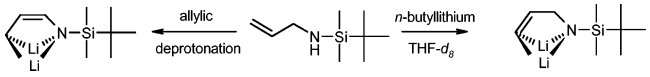

prediction is substantiated by the fact that in the structurally related allylic dianions derived from *N*-allyl-pivalamide[20] and *N*-(trialkylsilyl)but-3-en-1-amine,[32] the allylic lithiums were shown to be localized at the terminal carbon based on ^{13}C NMR chemical shifts (Scheme 4). In fact, comparison of the relative stabilities of the vinylic and allylic dianions of *N*-(trimethylsilyl)-

Scheme 4

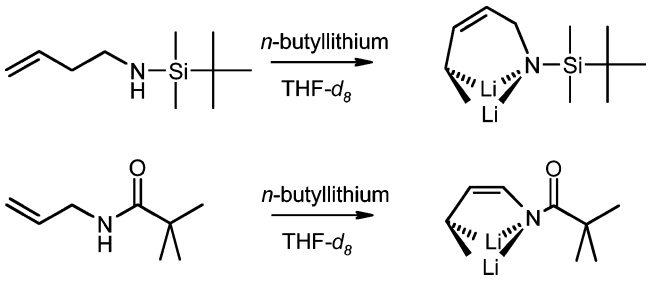

allylamine by computational methods (DFT//PM3)[29] suggests that the allylic dianion is preferred by a significant 8 kcal/mol.[33]

Furthermore, the *c*-clamp structure alone cannot explain why ethereal solvents are required for the reaction to proceed. While it is possible that ethereal solvation stabilizes the vinylic dianion in solution, we see no reason that a similar degree of stabilization could not be inferred to an allylic dianion. The fact that TBDMS and TIPS protected dianions crystallize[19] without solvating ether molecules strongly indicates that such solvation is not a prerequisite for the *c*-clamp.

Solution Structure of *N*-Lithio-*N*-(*tert*-butyldimethylsilyl)-allylamine (2). Since the structural characterization of the dianion did not furnish the answers we were seeking, we turned our attention to the reactants. The recent observation that lithium diisopropylamide forms a mixed aggregate with *n*BuLi in THF,[28] and reports in the literature that indicate that directed aromatic lithiations may involve mixed aggregates between the alkyllithium and the substrate,[1c,34] as well as recent reports identifying mixed aggregates as crucial intermediates in lithiation reactions,[3a,b,c,e] prompted us to investigate the aggregation behavior of **2** in detail.

All NMR samples used in this work were prepared by titrating **2** into NMR tubes containing 0.6 mL of a precooled 0.2 M solution of *n*BuLi in the appropriate solvent. THF-d_8 samples were maintained below −80 °C for the duration of the NMR experiments to prevent vinylic lithiation, which otherwise goes to completion within 2 h at room temperature. We detected no dianion formation at −80 °C by NMR, even after extended periods of observation.

Structure of 2 in THF-d_8. We found that in THF-d_8, **2** exists as an equilibrium mixture of THF solvated monomeric (**9**) and dimeric (**10** and **11**) aggregates (Scheme 5). In the presence of

Scheme 5

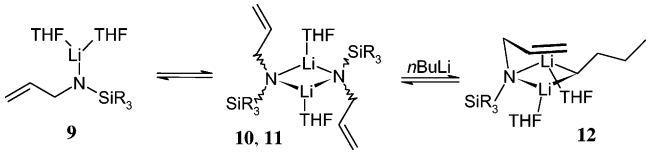

*n*BuLi, a THF solvated 1:1 mixed lithium amide/*n*BuLi dimer

(30) Keresztes, I.; Williard, P. G., manuscript in preparation.
(31) (a) Bauer, W. *J. Am. Chem. Soc.* **1996**, *118*, 5450−5455. (b) Mons, H. E.; Guenther, H.; Maercker, A. *Chem. Ber.* **1993**, *126*, 2747−2751.
(32) Jacobson, M. A.; Williard, P. G. *J. Org. Chem.* **2002**, *67*, 3915−3918.
(33) Single-point DFT calculations were performed using the pBP/DN** functional as implemented in PcSpartan Pro (Wave function Inc., Irvine, CA) on PM3 optimized geometries of unsolvated monomers of vinylic and allylic dianions of N-TBDMS allylamine.
(34) (a) Resek, J. E.; Beak, P. *J. Am. Chem. Soc.* **1996**, *116*, 405−406. (b) van Eikema Homes, N. J. R.; Schleyer, P. von R. *Tetrahedron* **1994**, *50*, 5903−5916. (c) Snieckus, V. *Chem. Rev.* **1990**, *90*, 879−933. (d) Beak, P.; Meyers, A. I. *Acc. Chem. Res.* **1986**, *19*, 356−363. (e) Klumpp, G. W. *Rec. Trav. Chim. Pays-Bas* **1986**, *105*, 1−21. (f) Gschwend, H. W.; Rodriguez, H. R. *Org. React.* **1979**, *26*, 1. (g) Wakefiled, B. J. *Chemistry of Organolithium Compounds*; Pergamon Press: Oxford, 1974. (h) Roberts, J. D.; Curtin, D. Y. *J. Am. Chem. Soc.* **1946**, *68*, 1658−1660.

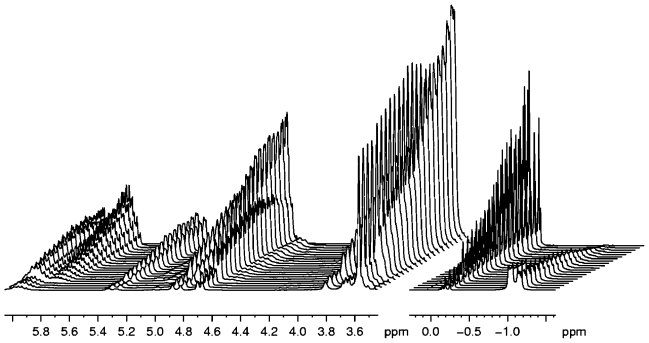

Figure 7. Titration of *n*BuLi with **2** in THF-d_8 at −80 °C. Downfield (left) and upfield (right) stacked expansion plots of ^{1}H NMR spectra with increasing lithium amide concentration from front to back.

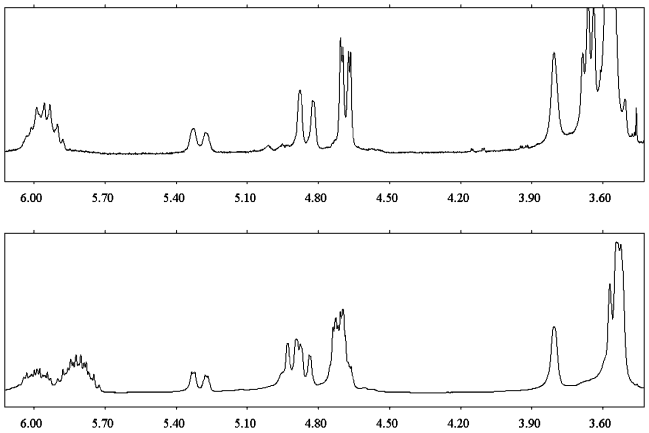

Figure 8. Titration of *n*BuLi with **2** in THF-d_8 at −80 °C. Expansion plots of the allylic region. Top: low lithium amide concentration (∼0.01 M). Bottom: high lithium amide concentration (0.2 M). Each spectrum was scaled independently.

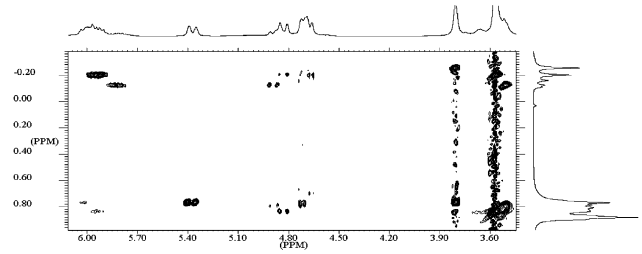

Figure 9. Phase-sensitive 2-D NOESY spectrum of a THF-d_8 solution 0.1 M each in **2** and *n*BuLi at −100 °C. Through-space correlations between the allylic resonances and the *t*-butyldimethylsilyl groups.

(**12**) is formed in addition to the homoaggregates. Evidence for these structures is presented next.

When the stepwise addition of **2** to *n*BuLi is followed by NMR at low temperatures (Figure 7), multiple sets of unique allylic resonances could be observed in the ^{1}H spectrum. At low lithium amide concentrations, two major sets of allylic resonances were observed. When all *n*BuLi is consumed, only one of these sets remains, along with two other major sets of resonances that are dominant at higher concentrations (Figure 8). Each set of resonances could be assigned to different lithium amide containing aggregates because their concentration profiles were unique during the titration.

Connectivity within the allylamine residues was confirmed for all four major aggregates by 2-D TOCSY (Figure 10) and NOESY experiments. NOESY also enabled us to extend the chemical shift assignments to the *t*-butyldimethylsilyl groups

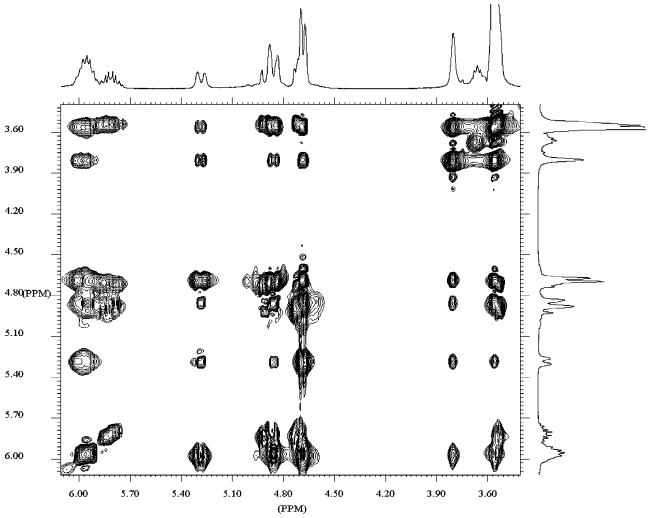

Figure 10. Phase-sensitive 2-D TOCSY spectrum of a THF-d_8 solution 0.1 M each in **2** and *n*BuLi at −100 °C. Correlations within the allyl groups via scalar coupling.

Table 3. ^{1}H/^{7}Li Chemical Shift Correlations[a] of Lithium Amide Containing Aggregates in THF-d_8 at −80 °C

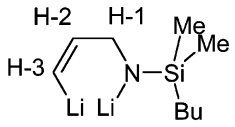

3

	4	**5**	**6**		**7**	**8**
H-1	0.95	1.80	N/D	H-1	1.36	N/D
H-2	0.95	1.86	N/D	H-2	0.79	0.78
H-3	0.95	1.82	1.38	H-3	0.79, 1.36	0.78, 1.48
				α-CH_2	0.79	0.21

[a] ^{7}Li chemical shifts in ppm.

Table 4. ^{1}H Chemical Shifts[a] of Lithium Amide Containing Aggregates in THF-d_8 at −100 °C

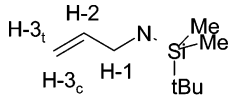

2

	lithium amide					*n*BuLi
	9	**10**	**11**	**12**		**12**
H-1	5.97	5.84	5.80	5.96	α	−1.14
H-2	5.29	4.91	4.86	4.85	*β*	1.34
H-3_c	4.69	4.71	4.73	4.69	*γ*	1.15
H-3_t	3.80	3.51	3.53	3.56	*δ*	0.82
*t*Bu	0.77	0.79	0.82	0.84		
Me	−0.26	−0.13	−0.11	−0.20	nOe[b]	−0.20

[a] In ppm, derived from 2-D TOCSY and NOESY experiments. [b] nOe correlation from *n*BuLi to lithium amide silyl methyl group.

(Figure 9). At −80 °C, nOe's were very weak and positive, but at −100 °C, nOe's were very strong and negative. Indeed, we had to use short mixing times to avoid spin diffusion and the resulting large number of indirect nOe correlations. Chemical shifts observed at −100 °C are summarized in Table 4.

The presence of lithium amide resonances that were predominant at low lithium amide concentrations but could not be observed in the absence of *n*BuLi strongly suggested the possibility of a mixed lithium amide/*n*BuLi aggregate. In

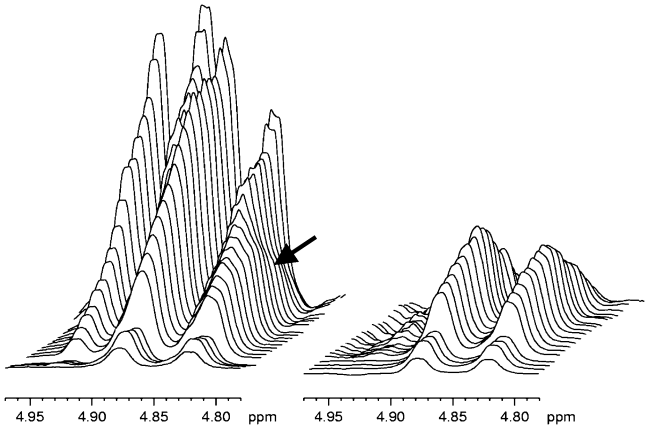

Figure 11. CVE of **2** and *n*BuLi in THF-d_8 at −80 °C. Left: stacked expansion plot of ^{1}H NMR spectra around the chemical shift of H-3$_c$ of the mixed aggregate with increasing lithium amide concentration. Arrow indicates the H-3$_c$ signal of the mixed aggregate. Right: stacked expansion plot of the H-3$_c$ resonance of the mixed aggregate after subtraction of the overlapping resonance.

addition, nOe correlations were observed between H-3$_c$ of **12** and the *n*BuLi β-CH_2 region, as well as the TBDMS methyl group of **12** and the α-CH_2 of the same *n*BuLi residue. We were able to derive more information about this mixed aggregate from the titration experiment. Titration of an alkyllithium with an amine is, in effect, a continuous variation experiment (CVE).[35,36] CVE's have been used to determine the stoichiometry of transition metal coordination complexes[37] and lithium enolates in complex mixtures.[38] In our case, the mole fraction profile of the mixed aggregate can be written[39] as

$$\eta_{\mathrm{mix}} = K(\eta_{\mathrm{LiN}})^m(1\eta_{\mathrm{LiN}})^n$$

While it was easy to determine the mole fraction of lithium amide by integration, the resonances of the suspected mixed aggregate were not well-resolved from those of other aggregates and thus could not be integrated directly. Fortunately, reliable quantitation of the H-3$_c$ resonance could be achieved by subtraction of the overlapping peaks (Figure 11) followed by integration. Fitting the experimental data yielded values for *n* and *m* that are consistent with a 1:1 mixed aggregate ($K = 0.6$, $m = 1.08$, $n = 1.09$) (Figure 12).

The composition of the mixed aggregate was confirmed, and aggregation numbers for the other three major lithium amide

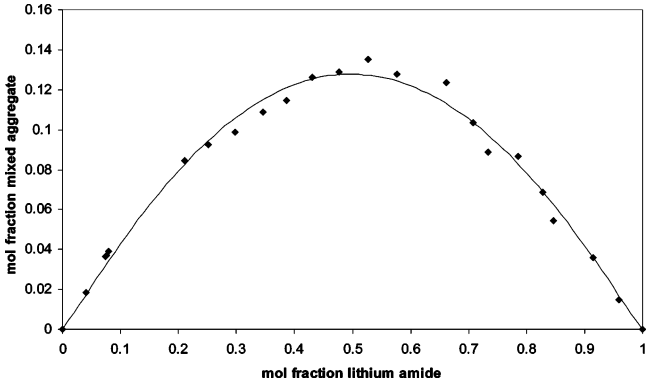

Figure 12. CVE of **2** and *n*BuLi in THF-d_8 at −80 °C. Job plot of mixed aggregate concentration as a function of total lithium amide concentration. The solid line represents the theoretical equation indicating a 1:1 lithium amide/*n*BuLi aggregate ($K = 0.6$, $m = 1.08$, $n = 1.09$).

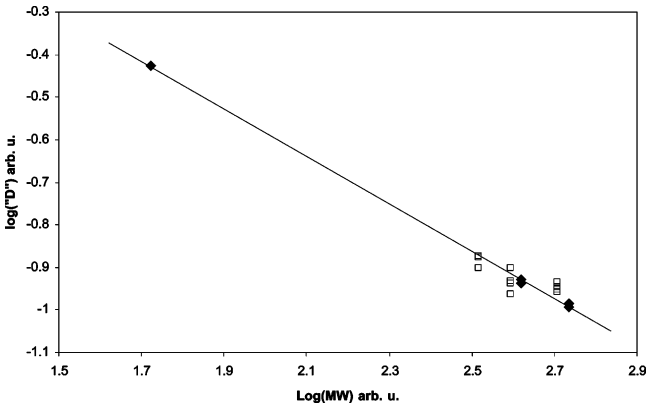

Figure 13. DO-NMR of the major aggregates in THF-d_8 at −80 °C. Diamonds represent reference compounds. The solid line is a linear least-squares fit to the reference points. Open squares represent lithium amide containing aggregates.

Table 5. DO-NMR of the Aggregates in THF-d_8 at −80 °C

	9	**10**	**11**	**12**	(*n*BuLi)$_4$	(*n*BuLi)$_2$
2	1	2	2	1	0	0
*n*BuLi	0	0	0	1	4	2
THF	2	2	2	2	4	4
MW	327	510	510	391	544	416

aggregates were determined by DO-NMR.[22] In this case, we used the well-known tetra-solvated dimeric and tetrameric nBuLi aggregates in conjunction with residual THF-d_7 as internal references to define a calibration curve. This curve was then used to determine the most likely composition for each of the lithium amide containing aggregates (Figure 13). Results are summarized in Table 5.

Structure of 2 in Toluene-d_8. In toluene-d_8, in addition to dimeric homoaggregates (**13**−**15**), the lithium amide **2** forms a mixed 1:3 lithium amide/*n*BuLi tetramer (**16**) (Scheme 6). Its concentration was considerably lower than the concentration of the 1:1 mixed aggregate in THF. Most ^{1}H chemical shifts for the major aggregates could be assigned by 2-D COSY and NOESY experiments and are summarized in Table 6. 2-D NOESY experiments recorded at −90 °C with a mixing time of 500 ms showed correlations between all resonances of the lithium amide molecule of the mixed aggregate and all resonances of the *n*BuLi residues, a clear indication that at this temperature the viscosity of toluene-d_8 is high enough to slow molecular tumbling to the point, where spin-diffusion is

(35) (a) Slovák, Z.; Borák, J. *Anal. Chim. Acta* **1974**, *68*, 425−434. (b) Likussar, W. *Anal. Chem.* **1973**, *45*, 1926−1931. (c) Klausen, K. S. *Anal. Chim. Acta* **1969**, *44*, 377−384. (d) Klausen, K. F.; Langmyhr, F. J. *Anal. Chim. Acta* **1963**, *28*, 335−340.

(36) In a CVE, the total concentration of the reactants is kept constant while the composition of the solution is varied and the concentration of the complex is recorded. The shape of this concentration profile provides information regarding the composition of the complex. In our case, the total lithium ion concentration remains unchanged throughout the reaction, and the molar composition of the solution changes from all alkyllithium to all lithium amide.

(37) (a) Likussar, W.; Boltar, D. F. *Anal. Chem.* **1971**, *43*, 1273−1277. (b) Likussar, W.; Boltz, D. F. *Anal. Chem.* **1971**, *43*, 1265−1272.

(38) McNeil, A. J.; Toombes, G. E. S.; Chandramouli, S. V.; Vanasse, B. J.; Ayers, T. A.; O'Brien, M. K.; Lobkovsky, E.; Gruner, S. M.; Marohn, J. A.; Collum, D. B. *J. Am. Chem. Soc.* **2004**, *126*, 5938−5939.

(39) The equilibrium formation of a binary mixed aggregate of unknown stoichiometry can be written as $m\mathrm{R_2NLi} + n\mathrm{R'Li} \rightleftharpoons (\mathrm{R_2NLi})_m(\mathrm{R'Li})_n$. The equilibrium constant for this reaction (K) can be rearranged to yield $[(\mathrm{R_2NLi})_m(\mathrm{R'Li})_n] = K[\mathrm{R_2NLi}]^m[\mathrm{R'Li}]^n$ or $[(\mathrm{R_2NLi})_m(\mathrm{R'Li})_n] = K[\mathrm{R_2NLi}]^m(\mathrm{Li_0} - [\mathrm{R_2NLi}])^n$, where $\mathrm{Li_0}$ is the total lithium ion concentration. Mol fractions can be substituted to give $\eta_{\mathrm{mix}} = K(\eta_{\mathrm{LiN}})^m(1\eta_{\mathrm{LiN}})^n$, where η_{mix} is the mol fraction of the mixed aggregate and η_{LiN} is the mol fraction of lithium amide.

Scheme 6

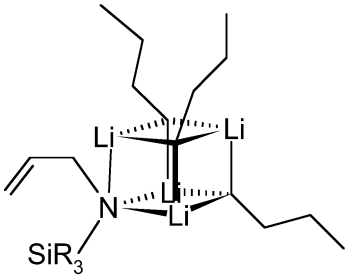

16

Table 6. [1]H Chemical Shifts[a] of Lithium Amide Containing Aggregates in Toluene-d_8 at −90 °C

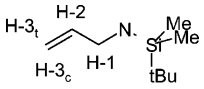

2

	lithium amide				*n*BuLi	
	13	**14**	**15**	**16**		**16**
H-1	N/D	3.60	3.54	3.56	α	−0.73
H-2	6.04	6.06	5.96	5.96	*β*	1.44
H-3_c	5.15	5.10	5.06	4.85	*γ*	1.63
H-3_t	N/D	4.96	4.91	4.69	*δ*	1.11
Bu		0.99−1.11[b]		0.84		
Me		0.06−0.25[b]		−0.20	nOe[c]	−0.20

[a] In ppm, derived from 2-D TOCSY and NOESY experiments. [b] Range for **13**, **14**, and **15**. Individual chemical shifts could not be determined. [c] nOe correlation from *n*BuLi to lithium amide silyl methyl group.

operational. Repeating the experiment with a 25 ms mixing time reduced the number of correlations sufficiently so that the primary nOe correlations could be identified (Figure 14). Unfortunately, peak overlap—even in 2-D spectra—made the unambiguous assignment of all resonances impossible. Strong nOe correlations were observed for **16** between H-1 and the α-CH_2 of *n*BuLi, as well as the α-CH_2 and the TBDMS methyl resonances. A weak correlation was observed between H-1 and the *β*-CH_2 of *n*BuLi.

The mixed aggregate **16** was identified based on (a) its concentration profile in a CVE, (b) its molecular weight, as determined by DO-NMR experiments, and (c) nOe correlations between allylic side chain and *n*BuLi resonances. The CVE experiment indicated that in this solvent the mixed aggregate contains one lithium amide residue and three molecules of *n*BuLi ($K = 0.24$, $m = 0.89$, $n = 2.88$) (Figure 15). Unfortunately, the concentration of **16** was very low, and its best resolved [1]H resonance was at the base of a much larger peak, making reliable quantitation difficult. Subtraction of a reference spectrum not containing the mixed aggregate followed by integration gave usable concentration data. The severe overlap in this spectrum also hindered the analysis of DO-NMR experiments, which require highly accurate quantitation. Data for overlapping resonances yield only the concentration-weighted average of the individual diffusion coefficients. Accordingly, the correlation between observed mobilities and MWs was considerably worse in this system than in the ones described earlier (Figure 16, Table 7).

Structure of 2 in Toluene-d_8 with 2 equiv of THF. The addition of small amounts of THF to a toluene-d_8 solution 0.1 M each in **2** and *n*BuLi brings about dramatic changes in the

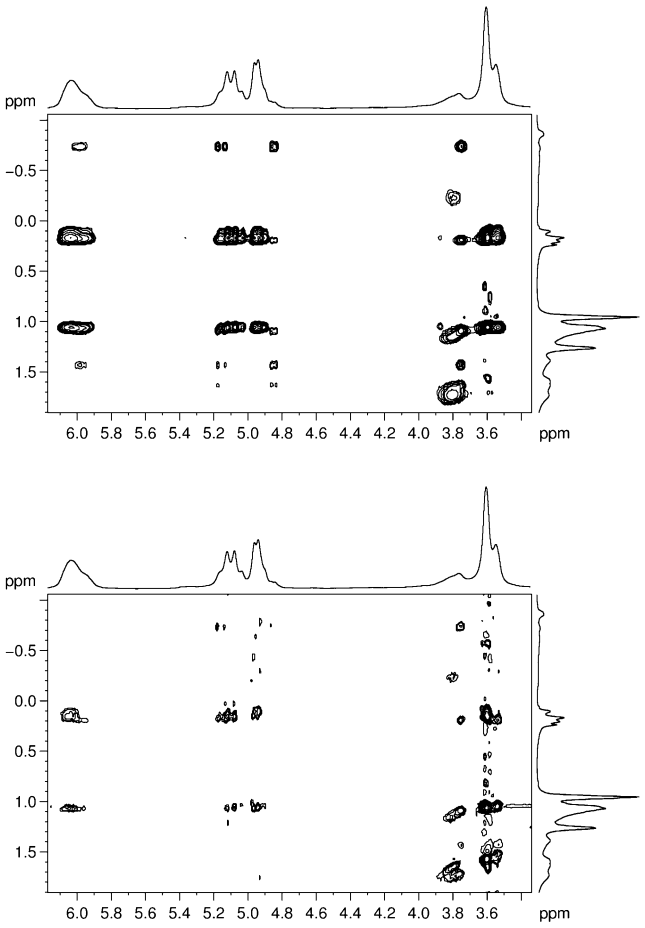

Figure 14. Phase-sensitive 2-D NOESY spectra of a toluene-d_8 solution 0.1 M each in **2** and *n*BuLi at −90 °C with varying mixing times (τ_m). Top spectrum $\tau_m = 500$ ms. Bottom spectrum $\tau_m = 25$ ms.

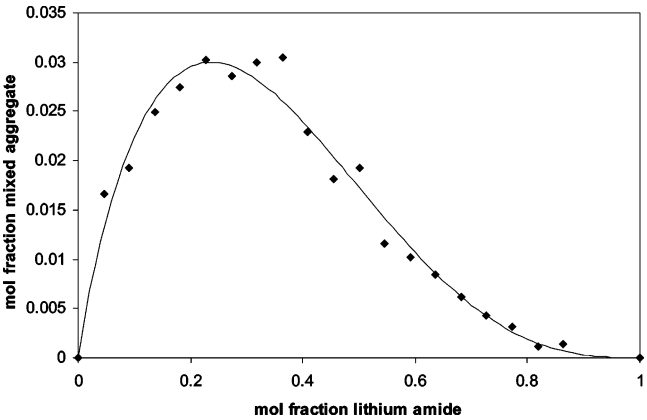

Figure 15. CVE of **2** and *n*BuLi in toluene-d_8 at −80 °C. Job plot of mixed aggregate concentration as a function of total lithium amide concentration. The solid line represents the theoretical equation indicating a 1:3 lithium amide/*n*BuLi aggregate ($K = 0.24$, $m = 0.89$, $n = 2.88$).

[1]H NMR spectrum (Figure 17). After the addition of 2 equivof THF, none of the amide peaks observed in neat toluene-d_8 were present. Instead, the vinylic region displayed only two sets of allyl resonances, and a new set of *n*BuLi peaks appeared at unique and new chemical shifts. These resonances were assigned to a THF solvated lithium amide homoaggregate (**17**) and the same 1:1 lithium amide/nBuLi mixed aggregate observed in neat THF (**12**). All chemical shifts were determined by 2-D NMR, and the results are summarized in Table 8.

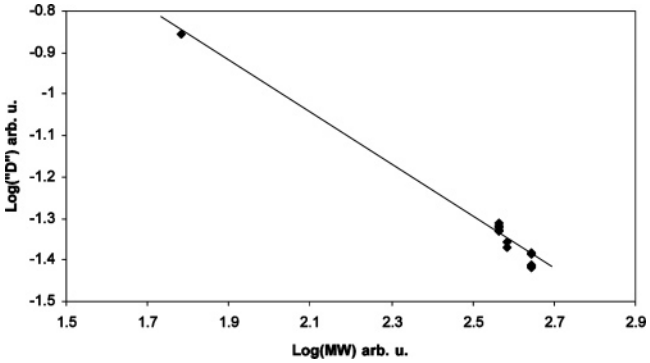

Figure 16. DO-NMR of the major aggregates at −90 °C. The solid line is a linear least-squares fit to all data points.

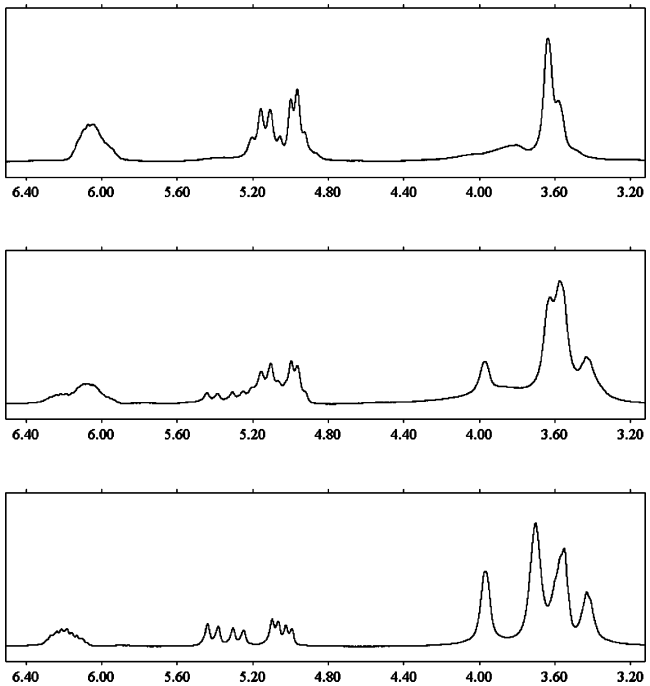

Figure 17. Downfield expansion plots of ^{1}H NMR spectra of a toluene-d_8 solution 0.1 M each in **2** and *n*BuLi at −80 °C with increasing THF concentrations from top to bottom (0, 2, and 4 μL, respectively).

Table 7. DO-NMR of the Aggregates in Toluene-d_8 at −90 °C

	13–15	16	$(n\text{BuLi})_6$
2	2	1	0
*n*BuLi	0	3	6
MW	386	375	384

Surprisingly, multiple peaks were also observed for the α- and β-CH_2 resonances of THF, indicating the presence of chemically nonequivalent THF molecules, which are slow to exchange on the NMR time scale. Observation of ether solvated aggregates at the slow ligand exchange limit was previously reported in the literature.[4d,40] All THF resonances had comprehensive sets of nOe correlations to one aggregate or the other, which allowed us to assign them to specific aggregates with certainty (Table 8). What came as a surprise to us was the observation that we could thus identify two chemically non-

(40) (a) Hilmersson, G. *Chem.—Eur. J.* **2000**, *6*, 3069−3075. (b) Reich, H. J.; Kulicke, K. J. *J. Am. Chem. Soc.* **1996**, *118*, 273−274. (c) Hilmersson, G.; Davidsson, Ö. *J. Org. Chem.* **1995**, *60*, 7660−7669. (d) Collum, D. B.; Lucht, B. L. *J. Am. Chem. Soc.* **1995**, *117*, 9863−9874. (e) Lucht, B. L.; Collum, D. B. *J. Am. Chem. Soc.* **1994**, *116*, 6009−6010.

Table 8. ^{1}H Chemical Shifts[a] of Lithium Amide Containing Aggregates in Toluene-d_8 Containing 2 equiv of THF at −90 °C

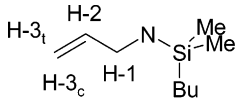

2

lithium amide			THF				*n*BuLi	
	17	**12**		**17**	**12**	**12**		**12**
H-1	3.94	3.39	α	3.52	3.67	3.39	α	−1.18
H-2	6.12	6.20				3.56	β	1.43
H-3_c	5.24	5.38	β	1.10	1.14	1.15	γ	1.18
H-3_t	4.98	5.05					δ	0.82
Bu	1.13	1.31						
Me	0.44	0.39						

[a] In ppm, derived from 2-D TOCSY and NOESY experiments.

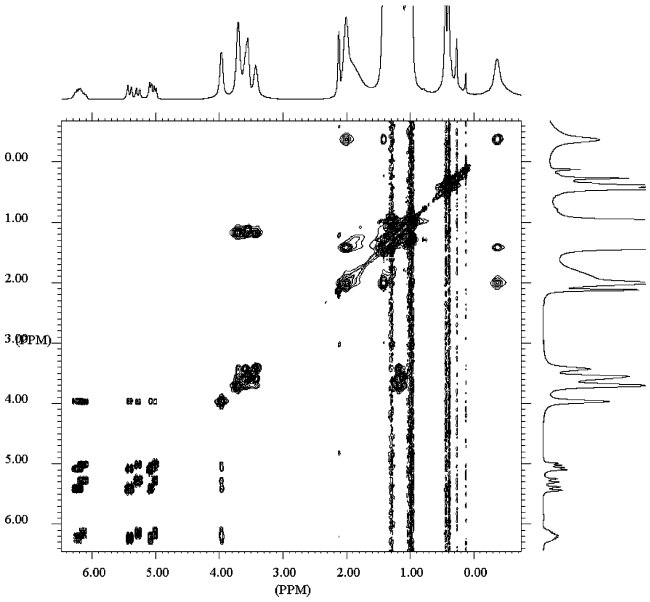

Figure 18. 2-D TOCSY spectrum of a toluene-d_8 solution 0.1 M each in **2** and *n*BuLi with 2 equiv of THF at −80 °C.

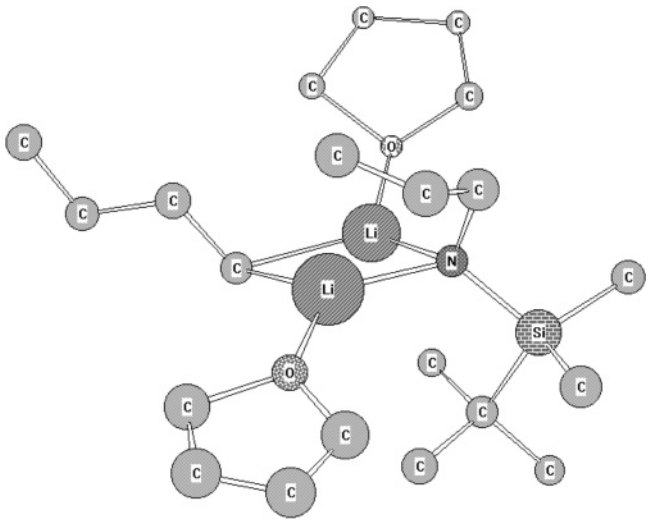

Figure 19. PM3 optimized structure of the THF solvated mixed aggregate **12**. Hydrogens were omitted for clarity.

equivalent THF molecules within a single aggregate (**12**). These THF molecules may undergo slow intraaggregate exchange as

Scheme 7. Proposed Mechanism for Vinylic Lithiation[a]

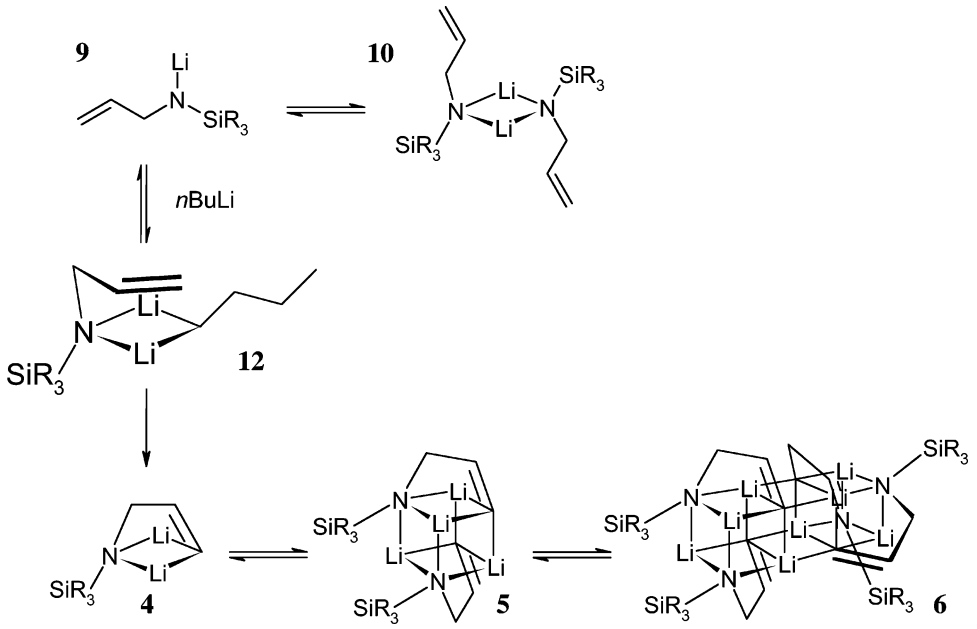

[a] Coordinating THF molecules omitted for clarity.

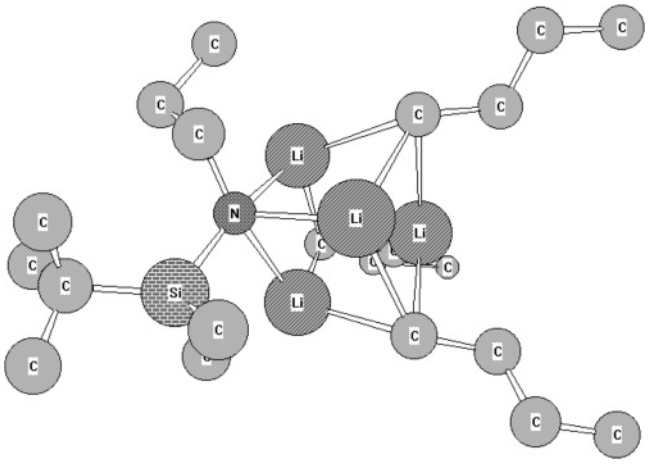

Figure 20. PM3 optimized structure of the mixed tetramer **16**. Hydrogens were omitted for clarity.

detected in 2-D NOESY experiments.[41] To the best of our knowledge, this is the first time that nonequivalent ethereal ligands attached to a single aggregate were directly observed by NMR. Furthermore, one of these THF molecules showed two nonequivalent α-CH_2 peaks, which are coupled to each other, as demonstrated by cross-peaks in COSY and TOCSY spectra (Figure 18).

Discussion

In THF solutions of **2**, in addition to the homoaggregates, a mixed aggregate, **12**, is formed that incorporates one molecule each of lithium amide and *n*BuLi. Molecular weight determination by DO-NMR suggested that the aggregate also incorporates two solvating THF molecules. The same THF solvated aggregate is generated when small amounts of THF are added to toluene solutions containing both **2** and *n*BuLi. Under these conditions, we could directly observe the two THF ligands, which are nonequivalent and may undergo slow intraaggregate exchange.

We were able to generate a detailed structure for the mixed aggregate **12** based on the available qualitative nOe data using PM3 semiempirical calculations,[29] which have been shown to predict equilibrium geometries of organolithium aggregates well.[29,42,] The central core of the aggregate is a four-membered ring made up of the α-carbon of a *n*BuLi molecule, the nitrogen of an amide, and two lithium atoms (Figure 19). Each lithium atom is also coordinated to a THF molecule. The substituents on the nitrogen are situated above and below the plane of the ring. The butyl chain, which has restricted rotation around the $\alpha-\beta$ bond as evidenced by the ^{1}H line shape of the α-CH_2 resonance, projects toward the same side of the central plane as the allyl group and opposite the side occupied by the bulky TBDMS group, as evidenced by nOe correlations between H-3_c and H-β, as well as the TBDMS methyl and H-α. The allyl chain is extended over the central ring of the aggregate toward the *n*BuLi residue, giving nOe correlation to the β-CH_2 resonance. The presence of nonequivalent THF molecules suggests that the allylic side chain likely coordinates to only one of the two lithium atoms. Close contacts indicative of bonding interactions between lithium atoms and olefins have been observed in numerous crystal structures.[43] The THF

(41) At 90 °C, nOe's are negative; thus, cross-peaks arising from spatial proximity (NOESY-type) and chemical exchange (EXSY-type) are indistinguishable.

(42) (a) Arvidsson, P. I.; Hilmersson, G.; Ahlberg, P. *J. Am. Chem. Soc.* **1999**, *121*, 1883−1887. (b) Hilmersson, G.; Arvidsson, P. I.; Davidsson, Ö.; Håkansson, M. *J. Am. Chem. Soc.* **1998**, *120*, 8143−8149. (c) Abbotto, A.; Streitweiser, A.; Schleyer, P. von R. *J. Am. Chem. Soc.* **1997**, *119*, 11255−11268. (d) Koch, R.; Wiedel, B.; Anders, E. *J. Org. Chem.* **1996**, *61*, 2523−2529. (e) Weiss, H.; Yakimansky, A. V.; Müller, A. H. E. *J. Am. Chem. Soc.* **1996**, *118*, 8897−8903. (f) Opitz, A.; Koch, R.; Katritzky, A. R.; Fan, W.-Q.; Anders, E. *J. Org. Chem.* **1995**, *60*, 3743−3749. (g) Pratt, L. M.; Khan, I. M. *J. Comput. Chem.* **1995**, *16*, 1067−1080.
(43) (a) Gauvin, R. M.; Kyritsakas, N.; Fischer, J.; Kress, J. *J. Chem. Soc., Chem. Commun.* **2000**, 965−966. (b) Eichhorn, B.; Noth, H.; Seifert, T. *Eur. J. Inorg. Chem.* **1999**, 2355−2368. (c) Veith, M.; Koban, A.; Huch, V. *Helv. Chim. Acta* **1998**, *81*, 1640−1644. (d) Dias, H. V. R.; Wang, Z. *J. Organmet. Chem.* **1997**, *539*, 77−85. (e) Niemeyer, M.; Power, P. P *Inorg. Chem.* **1996**, *35*, 7264−7272. (f) Hertkorn, N.; Kohler, F. H.; Muller, G.; Reber, G. *Angew. Chem., Int. Ed. Engl.* **1986**, *25*, 468−469.
(44) Haeffner, F.; Jacobsen, M. A.; Keresztes, I.; Williard, P. G. *J. Am. Chem. Soc.* **2004**, *126*, 17032−17039.

molecule that showed only a single peak for its α-CH_2 had nOe correlations to TBDMS and *n*BuLi resonances exclusively. This suggests that this THF is coordinated to the lithium that is not coordinated to the allyl chain. This THF is free to rotate around the lithium oxygen bond resulting in a single α-CH_2 signal despite the asymmetrical chemical environment. The second THF molecule that displays nonequivalent α-CH_2 resonances is coordinated to the same lithium atom as the allyl group, as indicated by nOe correlations to all groups including the vinylic resonances. The presence of the coordinated olefin might impede rotation around the lithium−oxygen bond, resulting in the nonequivalency of the α-CH_2 resonances. The α-CH_2 resonances could not be assigned because they show identical sets of nOe correlations, possibly due to chemical exchange.

In toluene-d_8, we identified a mixed lithium amide/*n*BuLi aggregate with a significantly different structure. This aggregate, **16**, contains one molecule of lithium amide and three molecules of *n*BuLi. We suggest that this aggregate is a cubic tetramer (Figure 20).[4c] Unfortunately, we know less about this structure than its counterpart in THF. We did, however, observe nOe correlation between H-1 of the lithium amide and the α- and *β*-CH_2 of the *n*BuLi residue. This suggests that the allyl chain is pointed away from the nearest *n*BuLi residues rather than toward them, as is the case in THF. It is not entirely clear to us why the allylic side chain does not adopt the same conformation in this aggregate as in **12**. However, the conformational changes at the lithium centers that occur upon conversion from a dimeric to a tetrameric aggregate may play an important role in preventing the reaction in the tetrameric aggregate.

These structures also help explain why allylic lithiation does not take place in either solvents. It appears that the scaffolding of the aggregates holds the *n*BuLi away from the H-1 hydrogens, preventing deprotonation from taking place in this fashion.

Our proposal for the reaction mechanism of vinylic lithiation is presented in Scheme 7. In this work, we furnished experimental evidence for all structures invoked in this scheme.

Summary

In the course of this work, we uncovered a wide variety of structural variations in the aggregation behavior of **3**. There is a single unifying feature in all structures: each molecule of **3** adopts the same *c*-clamp shape conformation. While it seemed attractive to suggest that the stability of the *c*-clamp is the driving force behind the regioselectivity of the lithiation, computational results predicted that *c*-clamp shaped allylic dianions would be substantially more stable than vinylic ones. Furthermore, the *c*-clamp structure does not explain why ethereal solvents are required for the reaction to proceed, and in fact, crystallographic data strongly indicate that ethereal solvation is not a prerequisite for the *c*-clamp.

Turning our attention to the solution state behavior of the intermediate monoanion **2**, we found that it forms mixed aggregates with *n*BuLi in both the ethereal solvent THF and the hydrocarbon solvent toluene. However, in toluene, the mixed aggregate does not allow close contact between the allylic side chain and the base. This fact signifies that, while mixed aggregates are important in these reactions, mixed aggregate formation in itself, does not necessarily facilitate reactivity. THF then catalyzes vinylic lithiation of allylamine not simply by promoting the formation of a mixed aggregate but rather by promoting the formation of a particular dimeric mixed aggregate, where steric congestion is reduced to allow the olefin of the lithium amide to interact very closely with the base. In fact, in the computed structure of the THF solvated mixed aggregate, the C−H bond that is cleaved in the reaction is perfectly aligned with one of the carbon lithium bonds of the four-membered central ring. It is also situated so that the *c*-clamp structure of the dianion can be formed at the same time lithiation occurs, which might contribute to lowering the activation energy for this reaction. We contend that preorganization of the reactants in this aggregate, in this fashion, is exclusively responsible for the regiochemical outcome of this reaction.

It is apparent from this work that detailed understanding of aggregate structure is essential in understanding the reactivity of organolithium reagents. It is noteworthy that, in this case, careful application of standard small molecule 2-D NMR methods provided all the information that was required in explaining the mechanism of this reaction.

Acknowledgment. This work was supported by PHS Grant GM-35982 and NSF Grant 0213381.

JA0479540